KFUPM
Journal of Undergraduate Research International

Diamond Open Access

Article
Control and Instrumentation Engineering

Enhancing 2-DOF Helicopter MIMO System Control using ZOA-Tuned Single Neuron PID Algorithm

Abdullah Aljuaid and Fadi Alyoussef*

Cite https://doi.org/10.64589/juri/221317

Submitted: November 26, 2025 **Revised:** March 05, 2026 **Accepted:** March 11, 2026

ABSTRACT

Traditional proportional–integral–derivative (PID) controllers are broadly employed in engineering. However, they perform poorly in complex, non-linear systems, and the single-neuron PID (SNPID) has been proposed as an alternative. Few studies have applied SNPID controllers to multi-input multi-output (MIMO) systems, and none has implemented this control technique experimentally on a 2-DOF helicopter—a system that is both complex and nonlinear. In this study, the SNPID settings were optimally computed using the Zebra Optimization Algorithm (ZOA). The proposed SNPID controller was compared with a conventional PID controller, with both controllers tuned by the ZOA to ensure a fair assessment. Real-time results indicate that the SNPID controller achieves greater stability and more accurate reference tracking than the PID controller, with an integral square error (ISE) of 4.7101×10^{-4} versus 5.7751×10^{-4} for the PID controller. Furthermore, when disturbances occur, the SNPID controller returns to the reference signal, whereas the PID controller cannot. These findings provide evidence that SNPID controllers outperform conventional PID controllers in MIMO systems.

Keywords: proportional–integral–derivative (PID) control, single-neuron PID (SNPID), two-degree-of-freedom (2-DOF) helicopter, multi-input multi-output (MIMO) systems; Zebra Optimization Algorithm (ZOA), real-time control

1. INTRODUCTION

Numerous industrial applications make extensive use of proportional-integral-derivative (PID) control owing to its simple structure and robustness.[1] However, traditional PID controllers have fixed coefficients, which can reduce their performance or even cause instability in dynamic, nonlinear systems.[2,3] To address this limitation, artificial neural networks (ANNs) have been proposed, as they can handle complex and dynamic systems by updating their weights. However, ANNs incur computational overhead and require substantial processing time owing to the training of many weights.[1,4] Moreover, stability depends on network size and the number of training iterations.[5] To combine the simplicity of a traditional PID controller and the adaptivity of an ANN, the single-neuron PID (SNPID) controller has been introduced. It constitutes the basic unit of a neural network in which PID coefficients are optimized by an ANN.[6] Numerous studies have investigated SNPID controllers with different optimization methods—for example, radial basis function (RBF),[7] extended Kalman filter (EKF),[5] and fuzzy logic[1]–though these have been primarily applied in single-input single-output (SISO) applications.

In this study, an SNPID controller was evaluated on a two-degree-of-freedom (2-DOF) helicopter MIMO system, which is a complex, nonlinear system with coupling effects. Although the SNPID controller has been tested on a 2-DOF helicopter using only simulation,[8] to the best of our knowledge, no real-time results have been reported for controlling a 2-DOF helicopter. The following are this study's primary contributions:

1. The SNPID controller parameters are tuned using the Zebra Optimization Algorithm (ZOA).
2. A real-time platform is used to test and assess the performance of the SNPID controller for the 2-DOF helicopter MIMO system, representing the first such demonstration reported in the literature.

The rest of this document is structured as follows: Section 2 presents the 2-DOF helicopter MIMO system. Section 3 describes the proposed control algorithm. Section 4 presents the ZOA. The findings and discussion are presented in Section 5, and the conclusions are presented in Section 6.

2. THEORY: 2-DOF HELICOPTER MIMO SYSTEM

In this study, the Quanser 2-DOF helicopter (known as Aero 2) was used as a dual-rotor helicopter, as shown in Figure 1 (a). The free-body diagram of the helicopter is shown in Figure 1 (b). This model allows for rotation about the z-axis and y-axis; therefore, only yaw and pitch movements are possible. The following is the expression for the equations of motion:

$$J_p\ddot{\theta} + D_p\dot{\theta} + K_{sp}\theta = \tau_p, \tag{1}$$

$$J_y\ddot{\psi} + D_y\dot{\psi} = \tau_y. \tag{2}$$

The torques τ_p and τ_y acting on the pitch and yaw axes are expressed as follows:

$$\begin{cases} \tau_{\mathrm{p}} = K_{pp}V_p + K_{py}V_y \\ \tau_y = K_{yp}V_p + K_{yy}V_y \end{cases}, \tag{3}$$

where J_p denotes the total moment of inertia for pitch, D_p denotes the pitch damping coefficient, K_{sp} denotes the pitch stiffness, K_{pp} denotes the torque thrust gain from the pitch rotor, K_{py} denotes the cross-torque thrust parameter between the pitch and yaw, V_p denotes the pitch voltage, and V_y denotes the yaw voltage.

3. CONTROL ALGORITHMS

3.1. PID Controller. The PID controller is entirely dependent on the error signal $e(k)$, which is calculated at the discrete time instant k, expressed as follows:

$$e(k) = r(k) - y(k), \tag{4}$$

where $r(k)$ is the desired reference signal and $y(k)$ is the actual output. The discrete-time PID digital form is expressed as follows:

$$u(k) = K_p x_1 + K_i x_2 + K_d x_3, \tag{5}$$

where x_1, x_2, and $x_3$are defined as:

$$\begin{cases} x_1 = e(k) - e(k-1) \\ x_2 = e(k) \\ x_3 = e(k) - 2e(k-1) + e(k-2) \end{cases}. \tag{6}$$

Here, x_1 denotes the proportional component, x_2 denotes the integral component, and x_3 denotes the derivative component. Furthermore, K_p, K_i, and K_d denote gain coefficients that govern the stability and performance of the system. These coefficients vary from system to system, so therefore require a tuning method to obtain optimal values.

3.2. Adaptive Single-Neuron PID. The proposed controller is an adaptive SNPID controller. It has the same simple structure as the PID controller (5) but differs in how K_p, K_i, and $K_{d.}$ are adaptively computed, along with the weights w_1, w_2, and w_3. The weights are computed as follows:

$$\begin{cases} w_1 = w(k-1) + \eta_p e(k)\, u(k-1)\, x_1 \\ w_2 = w(k-1) + \eta_i e(k)\, u(k-1)\, x_2 \\ w_3 = w(k-1) + \eta_d e(k)\, u(k-1)\, x_3 \end{cases}. \tag{7}$$

where η_p, η_i, and η_d denote the learning rates that govern the changes in the corresponding weight coefficients w_1, w_2, and w_3, respectively. These equations define the self-learning mechanism that produces the real controller output $u(k)$, expressed as follows:

$$u(k) = u(k-1) + K \sum_{i=1}^{3} w_i^{'}(k)\, x_i. \tag{8}$$

In (8), the controller uses the previous output $(u(k-1))$ and an incremental term. K denotes the scaling coefficient of the adaptive SNPID controller, and $w_i^{'}$ denotes the normalized weights, defined as follows:

$$w_i^{'}(k) = \frac{w_i}{\sum_{i=1}^{3} |w_i(k)|}. \tag{9}$$

Figure 2 shows the SNPID controller implemented in MATLAB. The controller parameters are computed using the ZOA, as described in the following section.

4. ZEBRA OPTIMIZATION ALGORITHM

Zebras are African animals that can run at high speeds when threatened. They exhibit two main behavioral traits in nature: food acquisition and formulating a safety plan against predators.[10] These two behaviors inspired the development of the ZOA. The mathematical representation of the ZOA population

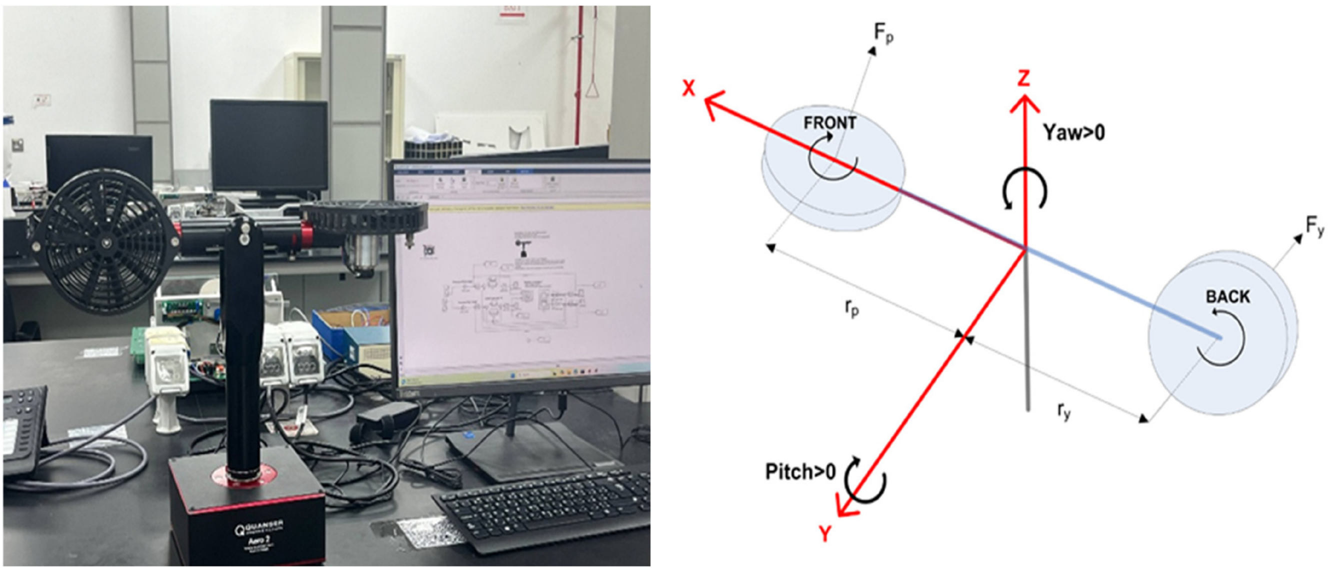

(a) (b)

Figure 1. (a) 2-DOF helicopter in the lab; (b) free-body diagram[9]

is expressed as follows:

$$X = \begin{bmatrix} X_1 \\ \vdots \\ X_i \\ \vdots \\ X_N \end{bmatrix}_{N\times M} = \begin{bmatrix} x_{(1,1)} & \cdots & x_{(1,j)} & \cdots & x_{(1,M)} \\ \vdots & \vdots & \vdots & \vdots & \vdots \\ x_{(i,1)} & \cdots & x_{(i,j)} & \cdots & x_{(i,M)} \\ \vdots & \vdots & \vdots & \vdots & \vdots \\ x_{(N,1)} & \cdots & x_{(N,j)} & \cdots & x_{(N,M)} \end{bmatrix}, \tag{10}$$

where X denotes the zebra population, X_i denotes the search agent of the i^{th} zebra, $x_{i,j}$ denotes the value for the j^{th} problem dimension of the i^{th} zebra, N denotes the number of search agents (zebras), and Mdenotes the dimensionality of the optimization problem. Each search agent represents a possible solution to the problem; consequently, the proposed values can be used to evaluate the objective function, expressed as follows:

$$F = \begin{bmatrix} F_1 \\ \vdots \\ F_i \\ \vdots \\ F_N \end{bmatrix}_{N\times 1} = \begin{bmatrix} F(X_1) \\ \vdots \\ F(X_i) \\ \vdots \\ F(X_N) \end{bmatrix}_{N\times 1}, \tag{11}$$

where F denotes the vector containing all F_i, which are the objective functions corresponding to X_i. The ZOA selects the lowest value in minimization or the highest value in maximization when comparing the objective function values. This strategy is repeated at each iteration. The two zebra behaviors are used to update the ZOA search agents; accordingly, the ZOA passes through two phases:

1. Food acquisition
2. Safety plan against predators.

Table 1. *PID coefficients*

Coefficient	Direction	Value
K_p	Pitch	999.15
K_i	Pitch	3.8995
K_d	Pitch	999.64
K_p	Yaw	959.12
K_i	Yaw	6.1865
K_d	Yaw	999.34

4.1. Phase 1: Food Acquisition Behavior. Zebras devote 60%–80% of their time to searching for their preferred food, which in many cases is grass. In the ZOA, the best search agent is called the pioneer zebra (PZ), which leads other agents toward its position in the search space. The mathematical formulation of the food acquisition phase is given in (12), and the updating condition is given in (13).

$$x^{new,P_1}_{(i,j)} = x_{(i,j)} + r\left(PZ_j - I \cdot x_{(i,j)}\right), \tag{12}$$

$$X_i = \begin{cases} X_i^{new,P_1}, & F_i^{new,P_1} < F_i \\ X_i, & else, \end{cases} \tag{13}$$

where X_i^{new,P_1} denotes the new position of the i^{th} zebra for phase 1, $x^{new,P_1}_{(i,j)}$ denotes its j^{th} dimension, $I = \text{round}\,(1 + \text{rand})$, with rand is an arbitrary number in the interval $[0, 1]$, F_i^{new,P_1} represents the objective function value, PZ_j represents the pioneer zebra in its j^{th} dimension, and r represents a random number in the interval $[0, 1]$.

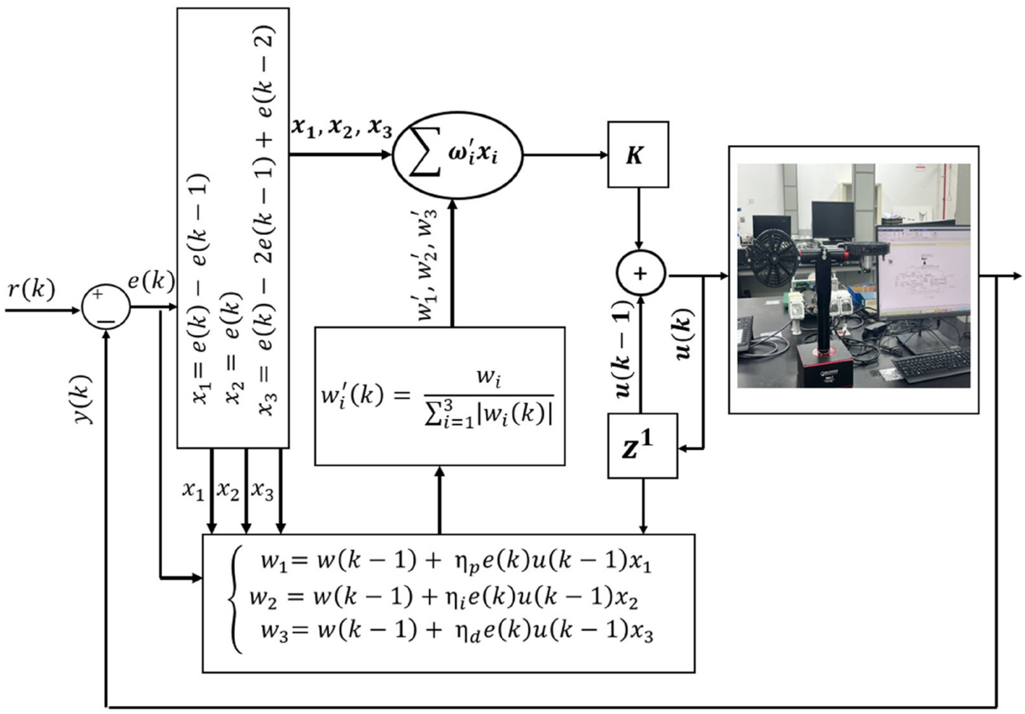

Figure 2. Schematic of the SNPID controller in MATLAB

4.2. Phase 2: Safety Plan Against Predators. While zebras graze, they face threats from various predators—for example, lions, leopards, hyenas, cheetahs, and wild dogs—with lions representing the primary threat. Zebras counter these threats through one of two strategies:

1. If the threat is a lion, the zebra attempts to escape.
2. If the predator is of another species, particularly a smaller one, the zebra would choose to confront and frighten it.

The two strategies are expressed mathematically in (14), and the updating condition is given as (15):

$$x_{(i,j)}^{new,P_2} = \begin{cases} S_1 : x_{(i,j)} + R\,(2r-1)\cdot\left(1-\frac{t}{T}\right), P_s \le 0.5 \\ S_2 : x_{(i,j)} + r\left(AZ_j - I\cdot x_{(i,j)}\right), else, \end{cases} \tag{14}$$

$$X_i = \begin{cases} X_i^{new,P_2}, & F_i^{new,P_2} < F_i; \\ X_i, & else, \end{cases} \tag{15}$$

where S_1 corresponds to the lion-threat scenario, S_2 corresponds to the other-predator scenario, X_i^{new,P_2} denotes the new position of the i^{th} zebra for phase 2, $x_{(i,j)}^{new,P_2}$ denotes its j^{th} dimension, F_i^{new,P_2} denotes its objective function value, t denotes the current step number, T denotes the total number of iterations (maximum number of iterations), R denotes a constant equal to 0.01, P_s denotes the probability of selecting a strategy, generated randomly in the interval [0, 1], and AZj denotes the position of a randomly selected zebra designated as the attacked zebra in the j^{th} dimension.

Table 2. *SNPID coefficients*

Coefficient	Direction	Value
K	Pitch	853.65
η_p	Pitch	0.0198
η_i	Pitch	0.0066
η_d	Pitch	0.0733
K	Yaw	858.19
η_p	Yaw	0.0672
η_i	Yaw	0.0047
η_d	Yaw	0.0534

5. RESULTS AND DISCUSSION

In this section, the PID and SNPID controllers are applied to the experimental platform. The coefficients for both controllers are tuned by the ZOA to ensure a fair comparison. Figure 3 shows the ZOA flowchart used to tune both controllers, in which the integral square error (ISE) is used as the objective function. In this study, the ISE is configured such that the ZOA minimizes the sum of the tracking errors on the pitch angle, e_p, and yaw

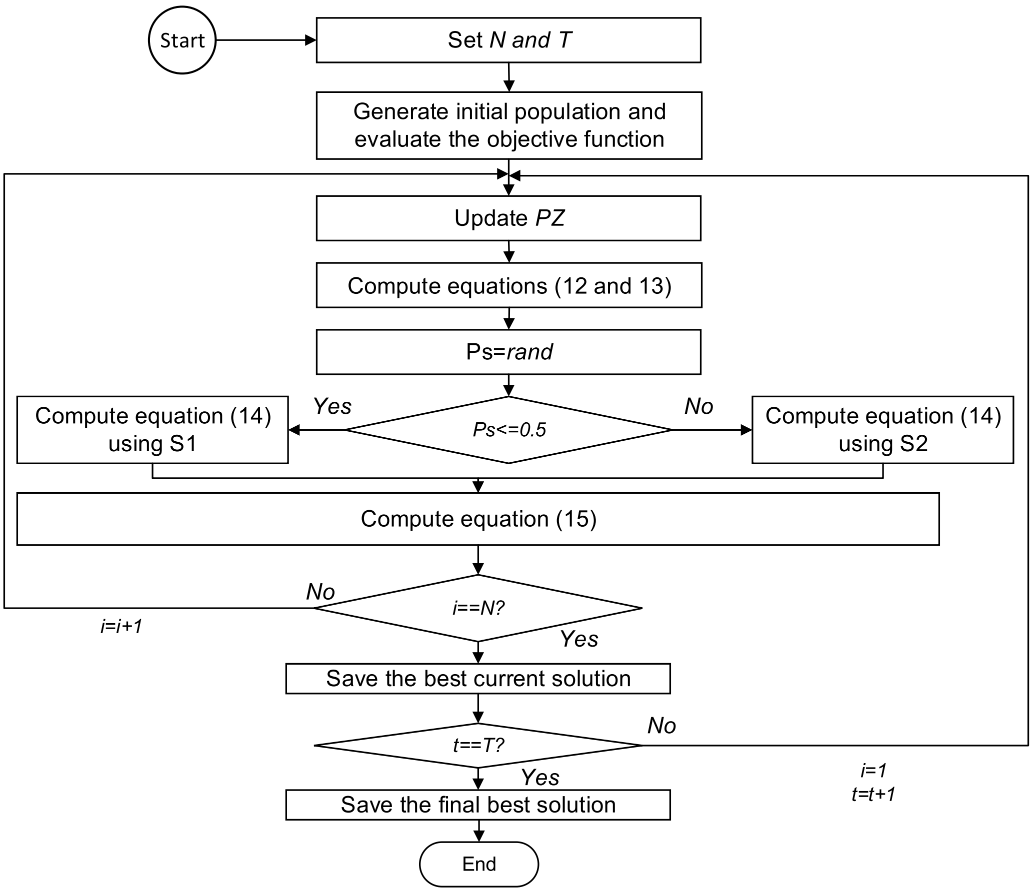

Figure 3. ZOA flowchart

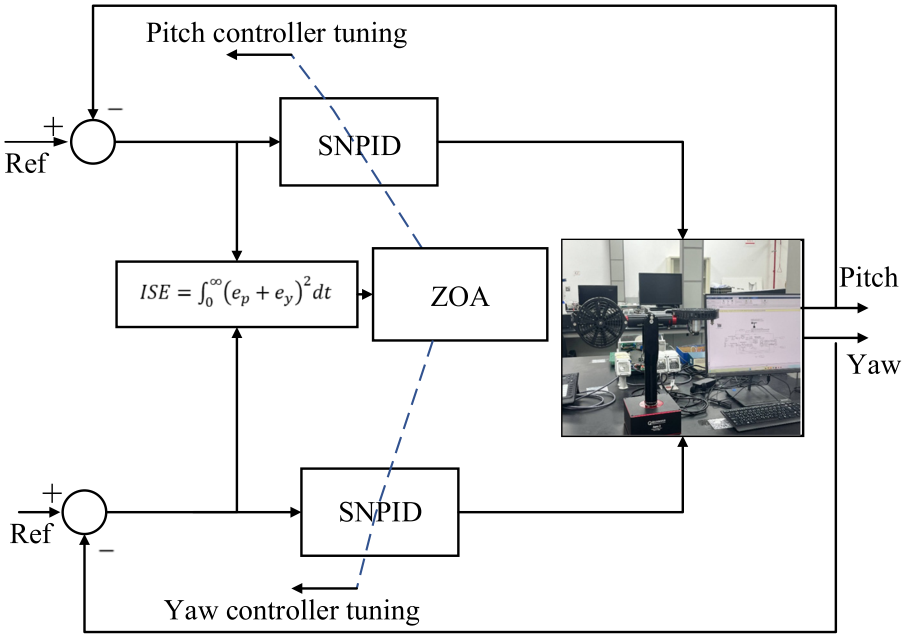

Figure 4. ISE computation

angle e_y. That is, the following ISE formulation is used: $ISE = \int_0^\infty (e_p + e_y)^2\, dt$.

Figure 4 illustrates the computation of the ISE for the proposed SNPID controller. Incorporating the total error in the pitch and yaw angles into the objective function implies that the ZOA must reduce the total error while accounting for the coupling effects. The system parameters and simulations were implemented using MATLAB R2024a. The ZOA optimization was performed offline; the resulting controller parameters were then used to obtain real-time results online.

5.1. Turing Coefficients. The PID coefficients (K_p, K_i, and K_d) were first optimized using the ZOA with $N = 100$ and $T = 30$. Figure 5 shows the convergence curve for the optimization process. The optimized coefficient values for both the pitch and yaw directions are listed in Table 1. To ensure a fair comparison, the optimized PID coefficients were used as initial values in the SNPID controller, the remaining coefficients (K, η_p, η_i and η_d), were then optimized using the same algorithm. The resulting ISE convergence curve is shown in Figure 6, and the corresponding coefficient values are presented in Table 2.

5.2. Experiments. In this experiment, the 2-DOF helicopter platform was used, as shown in Figure 1 (a), and the system was tasked with tracking a sinusoidal reference function. Figure 7 (a)and Figure 7 (b), show the pitch and yaw angle responses, respectively, with time on the x-axis, The SNPID controller achieves an ISE of 4.7101×10^{-4} compared with 5.7751×10^{-4} for the PID controller, demonstrating superior reference tracking.

Figure 7(c) and Figure 7(d) show the corresponding control signals; it is observed that the SNPID controller maintains a more consistent control signal, whereas the PID controller exhibits a more aggressive signal with larger oscillations. This suggests that the PID controller is more susceptible to noise than the SNPID controller, confirming that the SNPID controller is more stable in noisy environments. Similar performance was observed when the reference amplitude was increased to 30°: the ISE for the SNPID

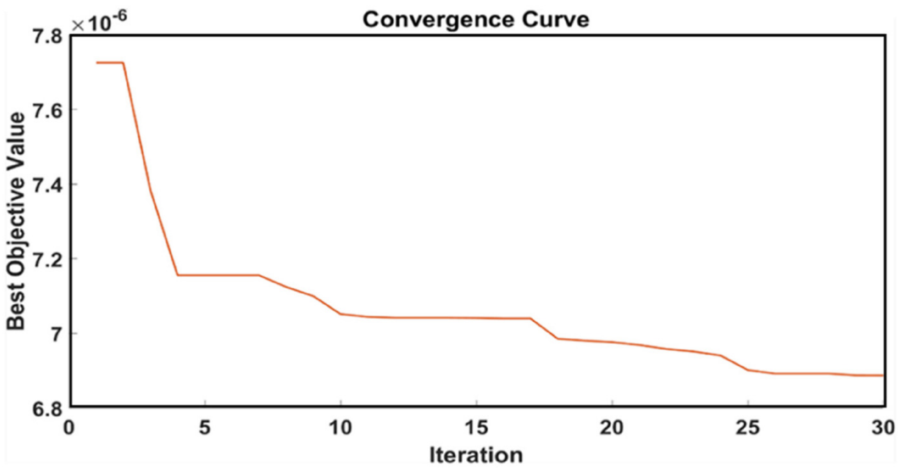

Figure 5. Integral square error of the Zebra Optimization Algorithm for PID coefficient tuning

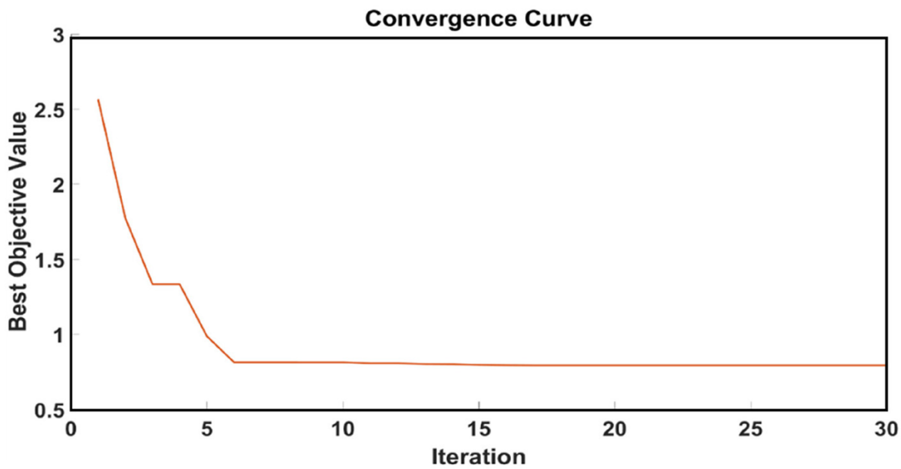

Figure 6. Integral square error of the Zebra Optimization Algorithm for SNPID coefficient tuning

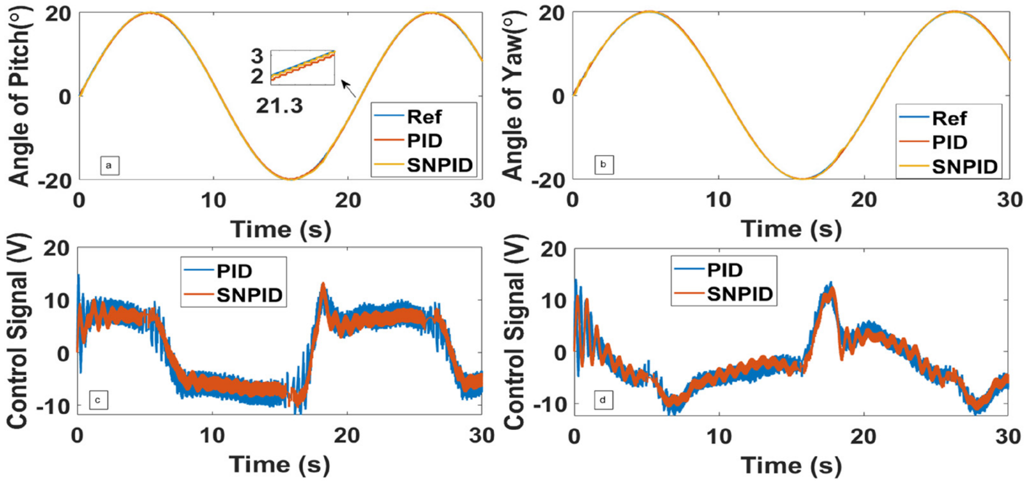

Figure 7. Sinusoidal reference tracking with an amplitude of 20° and a frequency of 0.05 Hz: (a) pitch response; (b) yaw response; (c) control signal for pitch; and (d) control signal for yaw

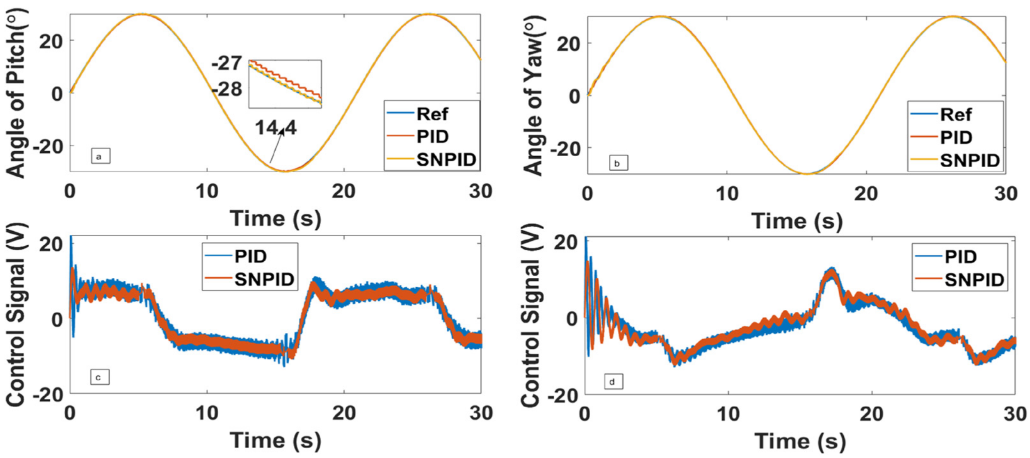

Figure 8. Sinusoidal reference tracking with an amplitude of 30° and a frequency of 0.05 Hz: (a) pitch response; (b) yaw response; (c) control signal for pitch; and (d) control signal for yaw

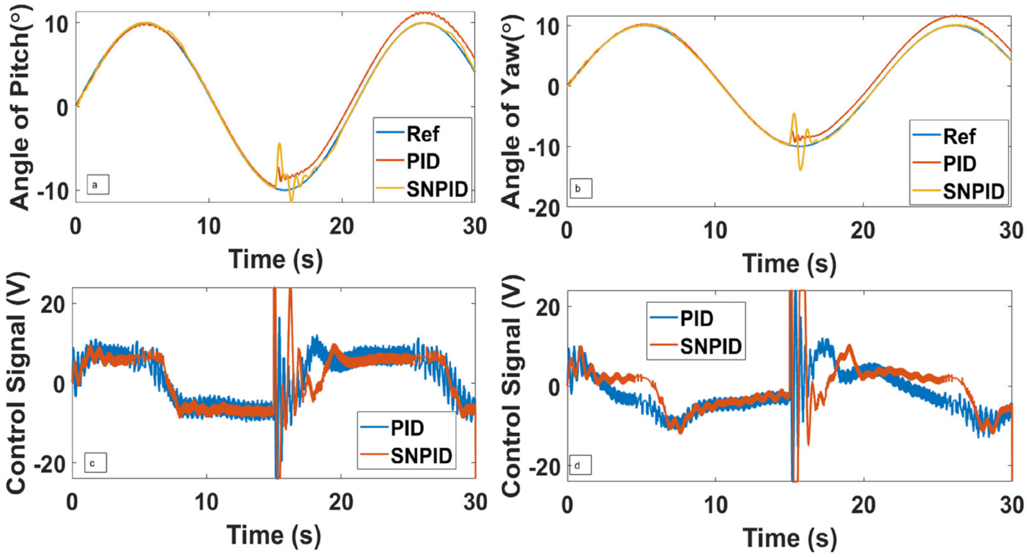

Figure 9. Sinusoidal reference tracking with an amplitude of 10° and a frequency of 0.05 Hz, subject to an internal disturbance in pitch and yaw with a magnitude of 10°: (a) pitch response; (b) yaw response; (c) control signal for pitch; and (d) control signal for yaw

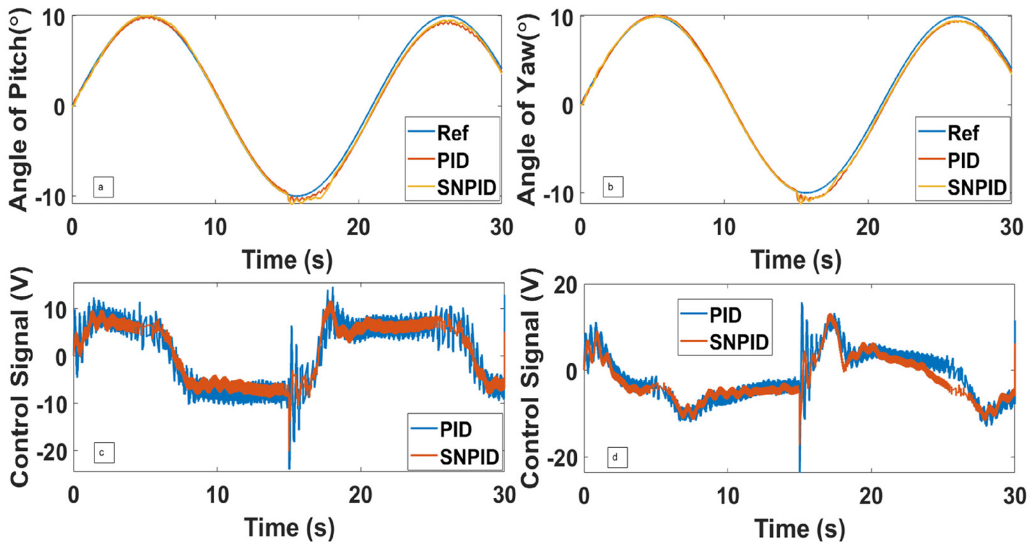

Figure 10. Sinusoidal reference tracking with an amplitude of 10° and a frequency of 0.05 Hz, subject to an external disturbance in yaw with a magnitude of 0.01 V: (a) pitch response; (b) yaw response; (c) control signal for pitch; and (d) control signal for yaw

controller was 5.4964×10^{-4} compared with 6.3272×10^{-4} for the PID controller. The SNPID controller continued to demonstrate the greatest stability and lowest tracking error, as shown in Figure 8.

Figure 9 presents results for a sinusoidal reference signal with an amplitude of 10 subject to an internal disturbance introduced at $t = 15$ s and persisting to the end of the trial. The ISE for the SNPID controller is 0.0075 compared with 0.018 for the PID controller. representing a substantially lower tracking error. When the disturbance was applied, the PID controller failed to return to the reference signal. By contrast, the proposed SNPID controller immediately rejected the disturbance and recovered the reference signal.

Figure 10 presents results for a sinusoidal reference signal with an amplitude of 10 subject to an external disturbance introduced at $t = 15$ s and persisting to the end of the trial. The ISE for the SNPID controller is 5.5053×10^{-4} compared with 6.1735×10^{-4} for the PID controller. When the disturbance was applied, the SNPID controller remained stable and provided more accurate tracking than the PID controller, as confirmed by the ISE values. However, neither controller fully recovered the original reference signal.

6. CONCLUSIONS

This study evaluated the performance of the SNPID controller in controlling an aerodynamic MIMO system. The results demonstrate that the SNPID controller exhibits a superior ability to track the reference signal in MIMO systems and to recover tracking after a disturbance, compared with the PID controller. These findings confirm the applicability of the proposed controller to MIMO systems in industrial applications, owing to its simple structure, making it a strong and practical competitor to the conventional PID controller. However, the selection of the initial weights affects the performance of SNPID. Therefore, future work will focus on developing methods to reduce this effect or to design these weights optimally.

AFFILIATIONS AND AUTHOR DETAILS

Undergraduate Author

Abdullah Aljuaid – *Department of Aerospace Engineering, King Fahd University of Petroleum & Minerals, Dhahran 31261, Saudi Arabia;* 0009-0005-6767-8195
Email: s202359630@kfupm.edu.sa

Corresponding Author

Fadi Alyoussef – *Research Mentor, Post Doctoral Fellow; Interdisciplinary Research Center for Aviation and Space Exploration, King Fahd University of Petroleum & Minerals, Dhahran 31261, Saudi Arabia;* 0000-0003-1878-1549
Email: fadi.youssef@kfupm.edu.sa

ACKNOWLEDGEMENTS

The authors would like to express their appreciation for the support received from the Department of Aerospace Engineering and the Interdisciplinary Research Center for Aviation and Space Exploration at King Fahd University of Petroleum and Minerals. Funding for this study was provided by the Undergraduate Research Office (URO), KFUPM, Saudi Arabia.

REFERENCES

(1) Zhou, X., Wang, J., Huang, L., Li, D. & Duan, Q. Modelling and controlling dissolved oxygen in recirculating aquaculture systems based on mechanism analysis and an adaptive PID controller. *Comput. Electron. Agric.* **192**, (2022).

(2) Ladjouzi, S. & Grouni, S. PID controller parameters adjustment using a single memory neuron. *J. Franklin Inst.* **357**, 5143–5172 (2020).

(3) Mendes, J., Osório, L. & Araújo, R. Self-tuning PID controllers in pursuit of plug and play capacity. *Control Eng. Pract.* **69**, 73–84 (2017).

(4) Kusumoputro, B. & Rifan, M. *Performance Characteristics of An Improved Single Neuron PID Controller Using Additional Error of an Inversed Control Signal. World Congress on Industrial Control Systems Security.*

(5) Hernandez-Barragan, J. *et al.* Adaptive single neuron anti-windup PID controller based on the extended Kalman filter algorithm. *Electronics (Switzerland)* **9**, (2020).

(6) Yang, Z. & Zhou, Q. A stability improvement control strategy research for LLC resonant converter with single neuron PI-I double closed loop control. *Ain Shams Engineering Journal* **15**, (2024).

(7) Zhang, M.-G. & Li, W.-H. *Single Neuron PID Model Reference Adaptive Control Based on RBF Neural Network.* (2006).

(8) *2009 IEEE/ASME International Conference on Advanced Intelligent Mechatronics: Suntec Convention and Exhibition Center, Singapore, July 14-17, 2009.* (IEEE, 2009).

(9) *Aero 2: Reconfigurable Dual-Rotor Aerospace Experiment for Controls Education and Research. [Online]. Available:* https://Www.Quanser.Com/Products/Aero-2/. *(2026)*

(10) Trojovska, E., Dehghani, M. & Trojovsky, P. Zebra Optimization Algorithm: A New Bio-Inspired Optimization Algorithm for Solving Optimization Algorithm. *IEEE Access* **10**, 49445–49473 (2022).